

## **Narrowing of the Upwelling Branch of the Brewer-Dobson Circulation and Hadley Cell in Chemistry-Climate Model Simulations of the 21<sup>st</sup> Century**

Feng Li<sup>1</sup>, Richard S. Stolarski<sup>2</sup>, Steven Pawson<sup>3</sup>, Paul A. Newman<sup>2</sup>, and Darryn Waugh<sup>4</sup>

<sup>1</sup>Goddard Earth Sciences and Technology Center, University of Maryland, Baltimore County, Baltimore, Maryland, USA

<sup>2</sup>Atmospheric Chemistry and Dynamics Branch, NASA Goddard Space Flight Center, Greenbelt, Maryland, USA

<sup>3</sup>Global Modeling and Assimilation Office, NASA Goddard Space Flight Center, Greenbelt, Maryland, USA

<sup>4</sup>The Johns Hopkins University, Baltimore, Maryland, USA

### **Popular Summary**

Strong evidence of a tropical belt expansion during the last three decades has been reported recently. Observational studies have shown that the Tropics have widened by more than two degrees latitude since 1979. Expansion of the Tropics in the 20<sup>th</sup> and 21<sup>st</sup> Century is also simulated by the Intergovernmental Panel on Climate Change (IPCC) Fourth Assessment Report (AR4) models. The widening of the Tropics is closely linked to the expansion of the Hadley cell's sinking branches. Because the Hadley cell's sinking branches cause the subtropical deserts, a widening of the Hadley cell means that the subtropical dry zones are moving toward more populated areas, including the American southwest, southern Australia and the Mediterranean basin. In addition, the tropical belt expansion is associated with changes in jet streams and storm tracks, and therefore has important implications in climate change. Understanding the mechanisms responsible for the tropical belt widening, particularly for the expansion of the Hadley cell, is an active research area.

This work investigates two important aspects of tropical expansion that have not been examined in previous studies. The first is the width of the stratospheric circulation (the Brewer-Dobson circulation) under global warming: it is important to understand whether tropical expansion extends into the stratosphere. The second topic is the width of the ascending branch of the Hadley cell: studying changes in the Hadley cell's upwelling will help to understand what causes the expansion of the Hadley cell's sink branch. These two topics were investigated using simulations of the 21<sup>st</sup> century from the Goddard Earth Observing System Coupled Chemistry Climate Model (GEOS CCM). The model results project a narrowing of the tropical upwelling region in the troposphere and lower stratosphere. However, the mechanisms for the narrowing of the upwelling branch of the Brewer-Dobson and the Hadley circulation are different. The narrowing of the upwelling of the Brewer-Dobson circulation in the lower stratosphere is due to the strengthening and equatorward shift of the subtropical jets, which enhances equatorward propagation of midlatitude eddies. On the other hand, the narrowing of the Hadley cell's ascending branch is caused by suppressed equatorward propagation of eddies, possibly a result of enhanced static stability in the troposphere. The reduced eddy wave activity causes anomalous eastward wave forcing in the subtropical upper troposphere, which drives an indirect circulation whose sinking branch narrows the tropical upwelling region.

# 1 Narrowing of the Upwelling Branch of the Brewer-Dobson Circulation and

## 2 Hadley Cell in Chemistry-Climate Model Simulations of the 21<sup>st</sup> Century

3

4 Feng Li<sup>1</sup>, Richard. S. Stolarski<sup>2</sup>, Steven Pawson<sup>2</sup>, Paul A. Newman<sup>2</sup>, and Darryn Waugh<sup>3</sup>

5

<sup>6</sup> <sup>1</sup>GEST, University of Maryland Baltimore County, Baltimore, MD

<sup>7</sup> NASA Goddard Space Flight Center, Greenbelt, MD

8 <sup>3</sup>Johns Hopkins University, Baltimore, MD

9

## Abstract

11 Changes in the width of the upwelling branch of the Brewer-Dobson circulation  
12 and Hadley cell in the 21<sup>st</sup> Century are investigated using simulations from a coupled  
13 chemistry-climate model. In these model simulations the tropical upwelling region  
14 narrows in the troposphere and lower stratosphere. The narrowing of the Brewer-Dobson  
15 circulation is caused by an equatorward shift of Rossby wave critical latitudes and  
16 Eliassen-Palm flux convergence in the subtropical lower stratosphere. In the troposphere,  
17 the model projects an expansion of the Hadley cell's poleward boundary, but a narrowing  
18 of the Hadley rising branch. Model results suggest that the narrowing of the Hadley cell  
19 ascent is also eddy-driven.

20

21

21    **1.    Introduction**

22            Strong evidence of a tropical belt expansion during the last three decades has been  
23    reported. Observational studies have shown that the Tropics have widened since 1979 by  
24    more than two degrees latitude – these studies use different empirical measures of the  
25    tropical width, such as the distance between the subtropical jets in the two hemispheres  
26    [*Hu and Fu*, 2007], the latitudinal range of tropical outgoing longwave radiation [*Hu and*  
27    *Fu*, 2007], and the subtropical tropopause height [*Seidel and Randel*, 2007]. Expansion of  
28    the Hadley circulation in the 20<sup>th</sup> and 21<sup>st</sup> Century is also simulated by the  
29    Intergovernmental Panel on Climate Change (IPCC) Fourth Assessment Report (AR4)  
30    models [*Lu et al.*, 2007]. The widening of the Tropics is associated with changes in the  
31    precipitation pattern, the hydrological cycle, jet streams, and storm tracks, and therefore  
32    has important implications in climate change [*Seidel et al.*, 2008]. Understanding the  
33    mechanisms responsible for the tropical belt widening, particularly for the expansion of  
34    the Hadley cell, is an active research area.

35            There are two important aspects of tropical expansion that have not been  
36    examined in detail in previous studies. The first is the width of the stratospheric tropical  
37    circulation under global warming. The stratospheric circulation in the Tropics is  
38    characterized by a slow, rising motion that forms the upwelling branch of the Brewer-  
39    Dobson circulation (BDC). The BDC plays a crucial role in the distribution of trace  
40    gases, such as ozone and water vapor, in the stratosphere. Because of its important  
41    implications for stratospheric ozone recovery, changes in the strength of the BDC in the  
42    21<sup>st</sup> Century have been extensively studied and nearly all middle-atmosphere models  
43    predict an acceleration of the BDC [*Butchart et al.*, 2006]. However so far there has been

44 no dedicated study on the width of the BDC. It is important to understand whether  
45 tropical expansion extends into the stratosphere and how the width change of the BDC is  
46 related to the strengthening of the BDC.

47 The second topic is the width of the ascending branch of the Hadley cell. Note  
48 that Hadley-cell widening refers to the expansion of its descending branch, which does  
49 not necessarily indicate a similar expansion of its ascending branch. Studying the width  
50 of the ascending branch of the Hadley cell may help to understand tropical expansion.

51 The purpose of this study is to investigate the response of the width of the  
52 upwelling branch of the BDC and Hadley cell to climate change in the 21<sup>st</sup> Century.  
53 Here, we use simulations from the Goddard Earth Observing System Coupled Chemistry-  
54 Climate Model (GEOSCCM) to show a narrowing of tropical upwelling in the lower  
55 stratosphere and troposphere.

56

## 57 **2. Simulations and Methods**

58 Details of the model used in this study, the GEOSCCM Version 1, are given in  
59 *Pawson et al.* [2008]. For this work, we analyzed two simulations of the 21<sup>st</sup> Century  
60 (2001-2099), referred to as FA1b and FA2, which used IPCC GHG scenarios A1b and  
61 A2. Data from FA1b and FA2 were used in several previous studies, including *Li et al.*  
62 [2009] and *Oman et al.* [2010]. For consistency with the GHG scenarios, the two model  
63 runs use single realizations of sea surface temperature (SST) and sea ice from appropriate  
64 AR4 scenarios run with the National Center for Atmospheric Research (NCAR)  
65 Community Climate System Model 3.0 (CCSM3). Both simulations use an identical

66 halogen scenario (WMO scenario AB) and all other external forcing is identical. Annual-  
67 mean results are presented in this study.

68 The BDC is the mean mass transport circulation in the stratosphere and it should  
69 be regarded as a Lagrangian mean circulation, but *Dunkerton* [1978] showed that the  
70 BDC could be approximated by the residual circulation under the Transformed Eulerian-  
71 Mean (TEM) frame. Here we use the latitudinal range of upward residual vertical  
72 velocity ( $\bar{w}^* > 0$ ) in the Tropics as a measure of the width of the BDC's upwelling  
73 branch.

74 We follow previous studies to investigate the Hadley cell under the conventional  
75 Eulerian-Mean (CEM) frame. The width of the Hadley cell is defined as the distance  
76 between its poleward boundaries, which are in turn defined as the latitudes where the  
77 zonal-mean mass streamfunction first becomes zero on the poleward side of its  
78 subtropical maxima [*Lu et al.*, 2007]. The width of the ascending branch of the Hadley  
79 cell is measured as the latitudinal range of tropical upwelling (vertical velocity  $w > 0$ ).  
80 Note that our model results regarding the narrowing of the Hadley cell's rising branch  
81 (section 4) do not change when analyzed under the TEM frame. We choose to use CEM  
82 to investigate Hadley cell change because the descending branch of the Hadley cell is not  
83 well defined in TEM.

84

### 85 **3. Narrowing of the Upwelling Branch of the BDC**

86 We focus on 70 hPa when investigating changes in the BDC in order to compare  
87 with previous studies [e.g., *Butchart et al.*, 2006]. Figure 1a shows the evolution through  
88 the 21<sup>st</sup> Century of the width and strength of the BDC's upwelling branch at 70 hPa in

89 FA1b and FA2. Despite different scenarios of GHG employed, the two simulations show  
90 the same long-time changes: narrowing and strengthening of the upwelling branch of the  
91 BDC.

92 The strengthening of the BDC has been extensively studied and our model results  
93 are consistent with other model results [e.g., *Butchart et al.*, 2009]. The trend of the BDC  
94 strength at 70 hPa in the 21<sup>st</sup> Century for FA1b is 1.33 %/decade, which is in the middle  
95 of the range predicted by eleven CCMs under the IPCC GHG A1b scenario [*Butchart et*  
96 *al.*, 2009]. But more interestingly for the purpose of this study, the FA1b and FA2 runs  
97 project a narrowing of the upwelling region at a rate of 0.41 and 0.61 degrees/decade  
98 (significant at the 95% confidence level). Although this change has been noted in recent  
99 studies [*McLandress and Shepherd*, 2009; *Li et al.*, 2009], it is not clear what causes this  
100 narrowing. Here we investigate the narrowing of the BDC in the lower stratosphere,  
101 using an analysis based on the downward control principle [*Haynes et al.*, 1991]. Since  
102 this behavior is very similar in both the FA1b and FA2 runs, the remainder of the analysis  
103 focuses on FA2.

104 The rising branch of the BDC is confined between the turnaround latitudes,  
105 defined as the locations where the residual vertical velocity ( $\bar{w}^*$ ) changes sign from  
106 tropical upwelling to extratropical downwelling. The turnaround latitudes correspond to  
107 the latitudes of the maxima and minima of the residual mass streamfunction ( $\Psi^*$ )  
108 because by definition  $\bar{w}^* = \frac{1}{\rho_0 a \cos \phi} \frac{\partial \Psi^*}{\partial \phi}$ , where  $\rho_0$  is the atmospheric density,  $a$  is the  
109 Earth's radius, and  $\phi$  is the latitude. The BDC is a wave-driven circulation, and  $\Psi^*$  can  
110 be approximated as

111

$$\Psi' = \int_z^{\infty} \frac{\rho_0 a^2 \cos^2 \phi}{\bar{m}} F dz' \quad (1)$$

112 under steady state conditions, where  $\bar{m}$  is the absolute angular momentum, and  $F$  is wave  
 113 forcing that consists of model-resolved wave and parameterized gravity-wave driving  
 114 [Haynes *et al.*, 1991]. Using the downward control analysis, we can diagnose what causes  
 115 the equatorward shift of the turnaround latitudes.

116 Figure 2a shows that at 70 hPa the climatological (2001-2020 mean) downward-  
 117 control and the actual residual streamfunctions have almost the same turnaround latitudes  
 118 and similar magnitudes. The downward-control residual streamfunction is dominated by  
 119 model-resolved wave forcing. At the turnaround latitudes ( $34^{\circ}\text{N}$  and  $36^{\circ}\text{S}$ ), resolved  
 120 waves and gravity waves account for 80% and 11% of the actual residual streamfunction,  
 121 respectively. The magnitude and the latitudinal structure of the trend in the downward-  
 122 control and actual residual streamfunctions also agree well with each other (Fig. 2b).  
 123 Comparing Figs. 2a and 2b reveals that the latitudinal distribution of the trend is shifted  
 124 toward the Equator compared to the climatological distribution. The maxima of the trend  
 125 are located at  $22^{\circ}\text{N}$  and  $20^{\circ}\text{S}$ , about  $15^{\circ}$  equatorward of the climatological turnaround  
 126 latitudes. Changes in the resolved-wave-driving streamfunction demonstrate similar  
 127 latitudinal shift and dominate changes in gravity wave forcing equatorward of  $30^{\circ}\text{N}$  and  
 128  $\text{S}$ . At the latitudes of maximum trend ( $22^{\circ}\text{N}$  and  $20^{\circ}\text{S}$ ), resolved wave and gravity wave  
 129 driving explain 81% and 9% of the actual trend, respectively. Based on the above  
 130 analyses, it is concluded that the narrowing of tropical upwelling in the lower  
 131 stratosphere is primarily due to increases in model-resolved wave driving in the  
 132 subtropics that shifts the EP flux convergence equatorward.

133 The increase in Rossby-wave driving in the subtropical lower stratosphere  
134 indicates enhanced wave propagation into this region (above 16 km in Fig. 2c). Rossby  
135 wave propagation is sensitive to changes in the basic state in the upper troposphere and  
136 lower stratosphere (UTLS) [e.g., *Garcia and Randel, 2008*]. Figure 2d shows the model  
137 simulated temperature trend in the 21<sup>st</sup> Century. GHG increases warm the troposphere  
138 and cool the stratosphere. The strongest warming occurs in the tropical upper  
139 troposphere; this enhances the meridional temperature gradient in the subtropical UTLS.  
140 Through thermal wind balance, the westerlies in the subtropical UTLS region strengthen  
141 (Fig. 2c). The largest westerly wind trends are located at about 30°N and S and 100 hPa  
142 (16 km), above and on the equatorward side of the subtropical jets, indicating an upward  
143 and equatorward shift of the jets. The strengthening and displacement of the subtropical  
144 jets has significant impacts on wave propagation. This may be explained qualitatively by  
145 the refractive index, which can be approximated as

$$146 \quad n_r^2 \approx \frac{\bar{q}_y}{\bar{u} - c}, \quad (2)$$

147 where  $n_r^2$  is the square of the refractive index,  $\bar{u}$  is the zonal-mean zonal wind,  $c$  is the  
148 eddy phase speed, and  $\bar{q}_y$  the meridional potential vorticity gradient. Rossby waves tend  
149 to propagate toward regions of large positive  $n_r^2$ , and are reflected away from regions of  
150 negative  $n_r^2$ . Therefore the equatorward propagation of mid-latitude waves is limited by  
151 the critical latitude, where the wave phase speed equals the zonal wind. The westerly  
152 acceleration in the subtropical lower stratosphere draws the critical latitude equatorward  
153 (for example, between 2001 and 2099 the zero wind lines at 70 hPa are displaced toward  
154 the Equator by about 3° of latitude in both hemispheres). As a result, the equatorward  
155 propagating extratropical eddies can penetrate deeper into the Tropics in the lower

156 stratosphere (above 16 km in Fig. 2c), shifting the EP flux convergence zone and the  
157 turnaround latitudes toward the Equator.

158

159 **4. Narrowing of the Upwelling of the Hadley Cell**

160 Readers should be remained that results presented in this section are calculated  
161 under the CEM frame. The width of the Hadley cell, diagnosed from the 500 hPa zero  
162 mass streamfunction, increases in the 21<sup>st</sup> Century in our model simulations (Fig. 1b).  
163 Our results are consistent with previous modeling studies [*Lu et al.*, 2007; *Johanson and*  
164 *Fu*, 2009]. *Lu et al.* [2007] reported a multi-model mean trend of 0.11 °/decade for the  
165 A1b scenario and 0.2°/decade for the A2 scenario from 15 IPCC AR4 models (estimated  
166 from their Figure 2), which are represented very well by the trends in our FA1b  
167 (0.11°/decade) and FA2 (0.14°/decade) simulations.

168 Figure 1b also shows that the width of the ascending branch of the Hadley cell  
169 (region of vertical velocity  $w > 0$ ) narrows, although in FA1b the narrowing is only  
170 statistically significant in the upper troposphere (300-200 hPa). This is the opposite  
171 behavior to the poleward expansion of the edge of the Hadley cell. The rate of the  
172 contraction of tropical ascent is smaller, but comparable to that of the expansion of the  
173 Hadley cell's poleward edges. This means that in the GEOSCCM the expansion of the  
174 sinking branches of the Hadley Cell occurs on both its poleward and equatorward flanks.

175 Again we focus on the FA2 run to investigate the mechanism for the narrowing of  
176 the Hadley rising branch. Figure 3a shows that trends of the vertical velocity are nearly  
177 symmetric between the hemispheres. In the subtropical middle-upper troposphere (4-10  
178 km), trends in the vertical velocity are opposite to its climatology mean, with increased

179 ascent in 20°S-35°S and 15°N-35°N and enhanced descent around 10°S-20°S and 10°N-  
180 15°N. The enhanced descent extends into the Tropics (more pronounced in the Southern  
181 Hemisphere), pushes the zero-vertical-velocity line equatorward, resulting in a narrowing  
182 of tropical upwelling. We suggest that this thermally indirect meridional circulation  
183 change is eddy-driven. Figure 3b shows that in the height range 8-12 km, the momentum  
184 flux convergence  $(-\frac{\partial \overline{u'v'}}{\partial y})$  increases at 10°-25° and decreases at 25°-50° in both  
185 hemispheres. These momentum flux convergence changes are caused by a reduced  
186 equatorward propagation of meridional eddy activity flux (the opposite of poleward eddy  
187 momentum flux) around 20°-40° latitudes in the height range 6-12 km (Fig. 3c). By  
188 applying westerly forcing in the subtropical upper troposphere, the increased momentum  
189 flux convergence drives a secondary indirect meridional circulation, which causes the  
190 narrowing of tropical upwelling (Fig. 3b). Our interpretation is inspired by *Seager et al.*  
191 [2003] who suggested that the mid-latitude cooling during El Niño events could be  
192 explained by anomalous ascent due to changes in an eddy-driven meridional circulation.

193 Now the question is what causes the upper tropospheric eddy flux changes. We  
194 note that the suppressed equatorward EP flux propagation between 20° and 40°N and S in  
195 the middle and upper troposphere (6-12 km) is accompanied by a reduction in the vertical  
196 component of the EP flux (Fig. 3c), that is, the direction of the EP flux trend is opposite  
197 to that of the climatological EP flux in this region (upward and equatorward, not shown).  
198 This observation suggests that suppression of wave propagation from the lower  
199 troposphere, due to changes in the background or source, might be a plausible  
200 explanation for the eddy flux changes in the upper troposphere.

201            We use refractive index to investigate how changes in the background state affect  
 202    wave propagation in the troposphere. We focus on the meridional potential vorticity (PV)  
 203    gradient (Equation 2), because the zonal-mean zonal wind trends are small below about  
 204    10 km (Fig. 2c) and changes in the refractive index are dominated by those in the PV  
 205    gradient (assume the eddy phase speed doesn't change). In the spherical coordinate, the  
 206    meridional PV gradient is

$$207 \quad \bar{q}_\phi = \frac{2\Omega}{a} \cos \phi - \frac{1}{a^2} \left[ \frac{(\bar{u} \cos \phi)_\phi}{\cos \phi} \right]_\phi - \frac{f^2}{\rho_0} \left( \rho_0 \frac{\bar{u}_z}{N^2} \right)_z, \quad (3)$$

208    where  $N$  is the buoyancy frequency,  $f$  is the Coriolis parameter, and other symbols have  
 209    their standard notations. A smaller PV gradient would suppress Rossby wave  
 210    propagation, and vice versa. Figure 3c shows a large area of decreased PV gradient below  
 211    about 9 km. The regions of decreased PV gradient coincide with reduced upward and  
 212    equatorward EP flux propagation. Expanding the right hand side of Equation 3 reveals  
 213    that the reduction in the PV gradient is mainly due to an increase in the static stability  
 214    (Fig. 3d). We conclude that changes in the basic state could be at least partly responsible  
 215    for the reduced wave propagation into the subtropical upper troposphere.

216            Another possible explanation for the suppressed wave activity in the subtropical  
 217    upper troposphere is a weakening of baroclinic eddy sources. *Frierson et al.* [2006] and  
 218    *Lu et al.* [2008] showed that an increase in static stability in the troposphere is a robust  
 219    response to global warming in AR4 simulations. They argued that the increased static  
 220    stability in the subtropics stabilizes the baroclinic growth rate and reduces eddy activity  
 221    there. The GEOSCCM simulates a significant increase of static stability in the subtropics  
 222    (Fig. 3d), and hence the decrease of equatorward and upward eddy fluxes between 20°

223 and 40° latitudes may be explained by the stabilization of eddies using the same argument  
224 of *Lu et al.* [2008].

225 The eddy wave activity changes in the troposphere may also be interpreted by  
226 changes in the wave phase speed. *Chen and Held* [2007] proposed that westerly  
227 accelerations in the UTLS would increase the eastward phase speed of tropospheric  
228 waves. Because faster waves have a more poleward-placed critical latitude, an increase in  
229 wave phase speed reduces equatorward wave activity fluxes in the subtropics and  
230 enhances wave activity in the mid-latitudes, leading to a poleward shift of the momentum  
231 flux convergence/divergence patterns: this is exactly what is shown in Figs. 3b and 3c.

232

233 **5. Discussion and Conclusions**

234 GEOSCCM simulations project a narrowing of the upwelling region in the  
235 tropical troposphere and lower stratosphere in the 21<sup>st</sup> Century. This work has examined  
236 mechanisms for the narrowing of the ascending branch of the BDC and Hadley cell. The  
237 equatorward and upward displacement of the subtropical jets, due to an enhanced  
238 meridional temperature gradient in the subtropical UTLS under global warming, causes  
239 an equatorward shift of the EP flux convergence zone and a narrowing of the upwelling  
240 in the lower stratosphere. Our results are consistent with *Garcia and Randel* [2008] and  
241 *McLandress and Shepherd* [2009] regarding the important role of increased subtropical  
242 wave forcing in causing changes in the BDC. *Garcia and Randel* [2008] and *McLandress*  
243 *and Shepherd* [2009] focused on the upward extension of the critical lines that leads to  
244 the strengthening of the BDC, but here we address the narrowing of the upwelling of the  
245 BDC and concentrate on the equatorward shift of the critical latitudes. These two aspects

246 of BDC changes are connected with each other. The key to understanding this connection  
247 is that Rossby waves tend to propagate toward regions of increased westerly winds in the  
248 subtropical lower stratosphere.

249 Our model results indicate that the narrowing of the Hadley rising branch is also  
250 eddy-driven. We argue that the subsidence of a subtropical secondary indirect circulation,  
251 driven by anomalous momentum flux convergence in the upper troposphere, pushes the  
252 boundary of the tropical ascent to move toward the Equator. Three possible mechanisms  
253 for the subtropical momentum flux convergence increase have been discussed: decreases  
254 in the refractive index that suppress wave propagation, stabilization of eddies due to an  
255 increased static stability, and increases in wave phase speed. Note that the last two  
256 mechanisms have been used to explain the expansion of the poleward boundaries of the  
257 Hadley cell [Lu *et al.*, 2008]. Therefore it is likely that the narrowing of the Hadley cell's  
258 ascending branch is closely related to the widening of the Hadley cell's descending  
259 branch.

260 Finally, we want to emphasize that the narrowing of the BDC is driven by  
261 enhanced EP flux convergence (easterly acceleration) in the lower stratosphere, whereas  
262 the narrowing of the Hadley's rising branch is due to increased momentum flux  
263 convergence (westerly acceleration) in the upper troposphere. These results are valid for  
264 the GEOSCCM using a single realization of SSTs from CCSM3. The robustness of our  
265 results needs to be verified with other CCMs and AR4 models. Of particular important is  
266 to identify how different representations of SSTs in CCMs (driven by SSTs from coupled  
267 models) and coupled atmosphere-ocean AR4 models influence tropical circulation  
268 response to global warming.

269 **Acknowledgements.** This work is supported by NASA's Modeling and Analysis  
270 program.

271

271 **References**

272 Butchart, N., and coauthors (2006), Simulations of anthropogenic change in the strength  
273 of the Brewer-Dobson circulation, *Clim. Dyn.*, 27, 727-741.

274 Butchart, N., and coauthors (2010), Chemistry-climate model simulations of 21<sup>st</sup> century  
275 stratospheric climate and circulation changes, *J. Clim.*, in press.

276 Chen, G., and I. M. Held (2007), Phase speed spectra and the recent poleward shift of  
277 Southern Hemisphere surface westerlies, *Geophys. Res. Lett.*, 34, L21805,  
278 doi:10.1029/2007GL031200.

279 Johanson, C. M., and Q. Fu (2009), Hadley cell widening: Model simulations versus  
280 Observations, *J. Clim.*, 22, 2713-2725.

281 Frierson, D. M. W., J. Lu, and G. Chen (2007), Width of the Hadley cell in simple and  
282 comprehensive general circulation models, *Geophys. Res. Lett.*, 34, L18804,  
283 doi:10.1029/2007GL031115.

284 Garcia, R. R. and W. J. Randel (2008), Acceleration of the Brewer-Dobson circulation  
285 due to increases in greenhouse gases, *J. Atmos. Sci.*, 65, 2731-2739.

286 Haynes, P. H., C. J. Marks, M. E. McIntyre, T. G. Shepherd, and K. P. Shine (1991), On  
287 the “downward control” of the extratropical diabatic circulation by eddy-induced  
288 mean zonal forces, *J. Atmos. Sci.*, 48, 651-678.

289 Hu, Y., and Q. Fu (2007), Observed poleward expansion of the Hadley circulation since  
290 1979, *Atmos. Chem. Phys.*, 7, 5229-5236.

291 Li, F., R. S. Stolarski, and P. A. Newman (2009), Stratospheric ozone in the post-CFC  
292 era, *Atmos. Chem. Phys.*, 9, 2207-2213.

293 Lu, J., G. A., Vecchi, and T. Reichler (2007), Expansion of the Hadley cell under global  
294 warming, *Geophys. Res. Lett.*, 34, L06805, doi:10.1029/2006GL028443.

295 Lu, J., G. Chen, and D. M. W. Frierson (2008), Response of the zonal mean atmospheric  
296 circulation to El Nino versus global warming, *J. Clim.*, 21, 5835-5851.

297 McLandress, C., and T. Shepherd (2009), Simulated anthropogenic changes in the  
298 Brewer-Dobson circulation, including its extension to high latitudes, *J. Clim.*, 22,  
299 1516-1540.

300 Oman, L. D., D. W. Waugh, S. R. Kawa, R. S. Stolarski, A. R. Douglass, and P. A.  
301 Newman (2010), Mechanisms and feedback causing changes in upper stratospheric  
302 ozone in the 21st century, *J. Geophys. Res.*, 115, D05303,  
303 doi:10.1029/2009JD012397.

304 Pawson, S., R. S. Stolarski, A. R. Douglass, P. A. Newman, J. E. Nielsen, S. M. Frith,  
305 and M. L. Gupta (2008), Goddard Earth Observing System chemistry-climate model  
306 simulations of stratosphere ozone-temperature coupling between 1950 and 2005, *J.*  
307 *Geophys. Res.*, 113, D12103, doi:10.1029/2007JD009511.

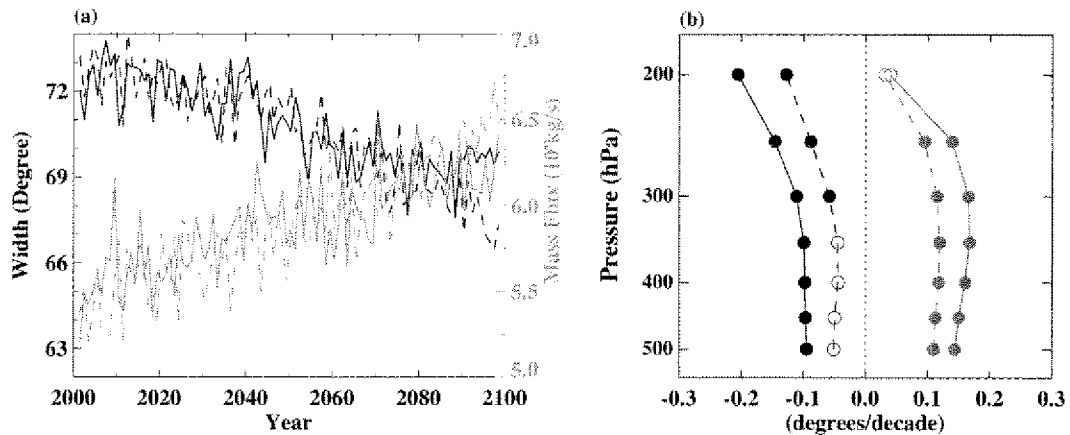
308 Seager, R., N. Harnik, R. Kushnir, W. Robinson, and J. Miller (2003), Mechanisms of  
309 hemispherically symmetric climate variability, *J. Clim.*, 16, 2960-2978.

310 Seidel, D. J., and W. J. Randel (2007), Recent widening of the tropical belt: Evidence  
311 from tropopause observations, *J. Geophys. Res.*, 112, D20113,  
312 doi:10.1029/2007JD008661.

313 Seidel, D. J., Q. Fu, W. J. Randel, T. J. Reichler (2008), Widening of the tropical belt in a  
314 changing climate, *Nature Geoscience*, 1, 21-24.

315  
316

316



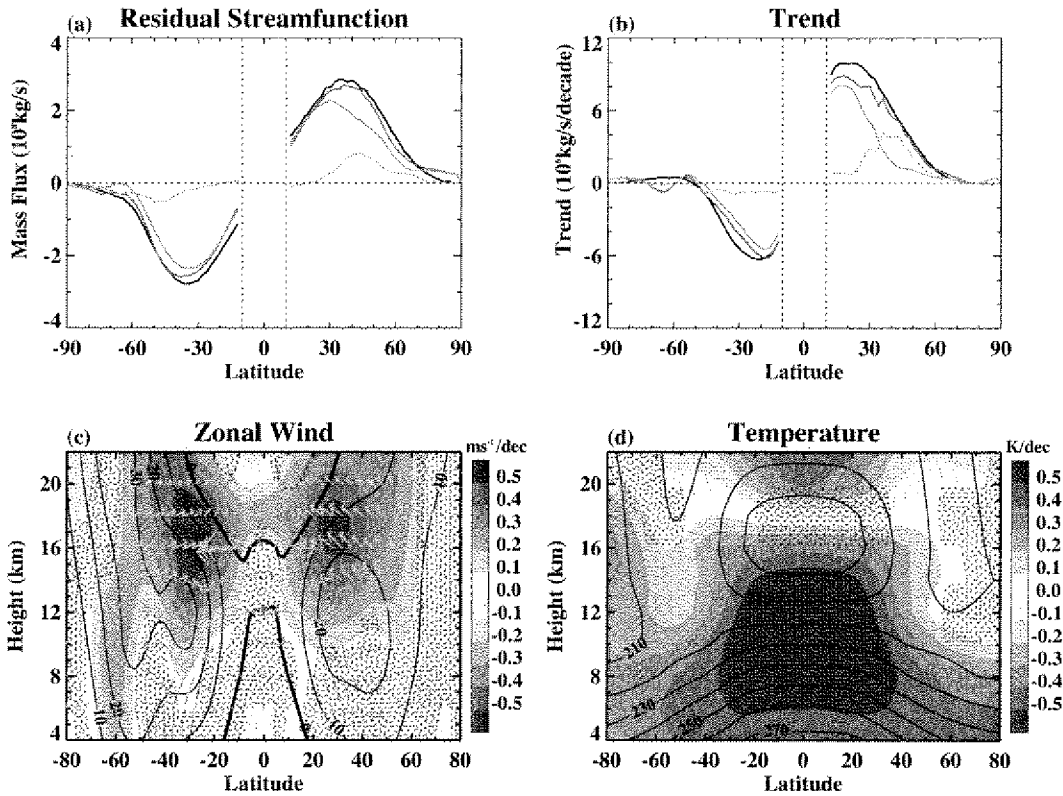
317

318 Figure 1: (a) Time series of the width of the BDC upwelling branch at 70 hPa (black, left  
319 axis), and the tropical upward mass flux at 70 hPa (blue, right axis). (b) Vertical profiles  
320 of the trends of the width of the Hadley cell poleward boundary (red) and the width of the  
321 Hadley rising branch (black). Filled circles indicate trends are statistically significant at  
322 the 95% confidence level. In both (a) and (b), solid and dashed lines are results from the  
323 FA2 and FA1b simulations, respectively.

324

325

325



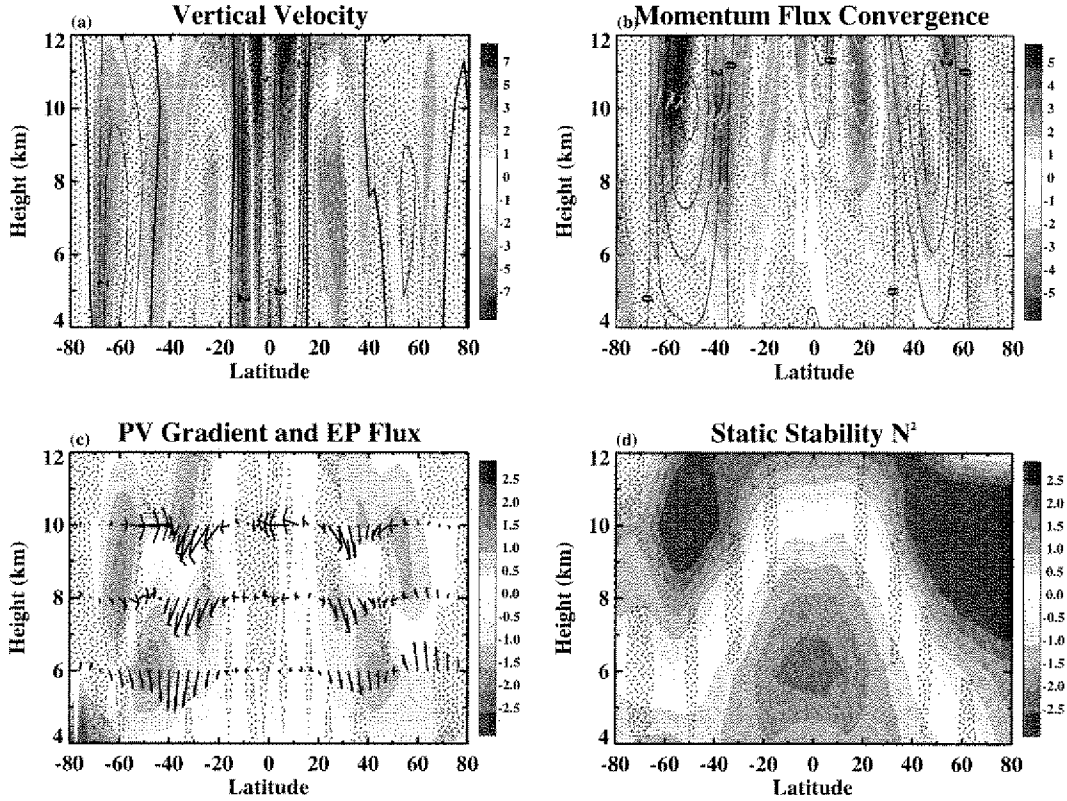
326

327 Figure 2: (a) Latitudinal distribution of the climatology (2001-2020 mean) of the actual  
 328 (black) and downward-control (red for combined resolved and gravity wave driving, blue  
 329 for resolved wave driving, and green for gravity wave driving) residual streamfunction at  
 330 70 hPa. (b) Same as (a), but for the trend in the 21<sup>st</sup> Century. (c) Trends of the zonal wind  
 331 in the 21<sup>st</sup> Century (shading). Stippling indicates that trends are not statistically  
 332 significant at the 95% confidence level. Contours are 2001-2020 mean. Arrows denote  
 333 trends in the EP flux. (d) Same as (c), but for the temperature. Results are from FA2.

334

335

335  
336



337

338

339 Figure 3: Trends in the 21<sup>st</sup> century of (a) the vertical velocity ( $10^{-5}\text{ms}^{-1}/\text{decade}$ ), (b) the  
340 momentum flux convergence,  $-\frac{\partial \bar{u}'v'}{\partial y}$  ( $10^{-2}\text{ms}^{-2}/\text{decade}$ ), (c) the meridional potential  
341 vorticity gradient ( $10^{-12}\text{m}^{-1}\text{s}^{-1}/\text{decade}$ ), and (d) the buoyancy frequency squared ( $10^{-4}\text{s}^{-2}/\text{decade}$ ). Stippling indicates that trends are not statistically significant at the 95%  
342 confidence level. Contours in (a) and (b) are 2001-2020 mean values (black for positive  
343 and white for negative values). Arrows in (b) and (c) denote trends in the meridional  
344 circulation and EP flux, respectively. Results are from FA2.  
345

346